

Shears Mechanism in the $A \sim 110$ Region

R. M. Clark,¹ S. J. Asztalos,¹ B. Busse,¹ C. J. Chiara,² M. Cromaz,¹ M. A. Deleplanque,¹ R. M. Diamond,¹ P. Fallon,¹ D. B. Fossan,² D. G. Jenkins,³ S. Juutinen,⁴ N. Kelsall,³ R. Krücken,^{1,*} G. J. Lane,² I. Y. Lee,¹ A. O. Macchiavelli,¹ R. W. MacLeod,¹ G. Schmid,¹ J. M. Sears,² J. F. Smith,^{2,†} F. S. Stephens,¹ K. Vetter,¹ R. Wadsworth,³ and S. Frauendorf⁵

¹Lawrence Berkeley National Laboratory, Berkeley, California 94720

²Department of Physics, SUNY at Stony Brook, Stony Brook, New York 11794

³Department of Physics, University of York, Heslington, York, YO1 5DD, United Kingdom

⁴Department of Physics, University of Jyväskylä, Jyväskylä, Finland

⁵Institut für Kern- und Hadronenphysik, Forschungszentrum Rossendorf, PF 510119, D-01314 Dresden, Germany

(Received 13 July 1998)

Lifetimes of states in a rotational-like $M1$ band in ^{110}Cd have been determined through a Doppler-shift attenuation method measurement performed with the Gammasphere array. The deduced $B(M1)$ values, which agree well with the predictions of the tilted axis cranking model, clearly confirm that it has the character of a shears band. Using a semiclassical scheme of the coupling of two long j vectors we deduce information on the strength and form of the effective interaction between the constituent nucleons. These results are the first definitive evidence of the shears mechanism and “magnetic rotation” in this mass region. [S0031-9007(99)08994-2]

PACS numbers: 27.60.+j, 21.10.Re, 21.10.Tg, 23.20.Lv

It has been suggested that sequences of magnetic-dipole ($M1$) transitions observed in light-Pb nuclei [1–4] can be regarded as a novel mode of nuclear excitation known as the “shears mechanism.” The interpretation of the bands involves high- Ω proton configurations ($h_{9/2}$ and $i_{13/2}$ orbitals coupled to \mathbf{j}_π) and low- Ω $i_{13/2}$ neutron holes (coupled to \mathbf{j}_ν). Calculations using a tilted-axis-cranking (TAC) model [5] show that the total angular momentum is generated almost completely by the recoupling of the proton and neutron vectors, \mathbf{j}_π and \mathbf{j}_ν . At the bandhead, \mathbf{j}_π and \mathbf{j}_ν are approximately perpendicular to each other. Higher angular momentum states are generated by aligning the two spin vectors in a way that resembles the closing of the blades of a pair of shears—hence, the name “shears bands” [6]. This coupling of proton particles and neutron holes results in a large magnetic dipole moment (μ), the perpendicular component (μ_\perp) of which decreases in a characteristic manner as \mathbf{j}_π and \mathbf{j}_ν align (and the total spin increases). The $B(M1)$, which is proportional to μ_\perp^2 , should then also decrease in a characteristic way. After several earlier efforts [7–10], recent lifetime measurements confirm this prediction and provide clear evidence that the $M1$ bands in $^{193-199}\text{Pb}$ can be best explained in terms of the shears mechanism [11–13].

The member states in these Pb shears bands follow a rotational-like behavior with the excitation energies following the pattern of $\Delta E(I) = E(I) - E(I_b) \sim A(I - I_b)^2$, where I is the spin of the state and I_b is the spin of the bandhead. However, the bands are based on weakly deformed oblate shapes ($|\epsilon_2| < 0.1$), and the interesting question has arisen as to why such weakly deformed structures should have such striking rotational-like properties? A new form of quantized rotation known as “magnetic rotation” [14] has been suggested

as a possible explanation. Unlike the familiar notion of nuclear rotation, arising when an intrinsic deformation breaks the spherical symmetry, it is the anisotropic arrangement of nucleon currents (which also give rise to the “blades” of the shears) that is responsible for the symmetry breaking. A related explanation, starting from a different point of view, has been suggested in terms of a residual interaction between the proton and neutron blades [15] that may arise from a particle-vibration coupling [16].

Long sequences of $M1$ transitions have also been observed in several nuclei of the Cd-Sn region with $A \sim 110$ [17–23]. These cascades share several characteristics with the bands in the Pb nuclei: (1) The states follow a rotational-like behavior; (2) the structures are thought to be based on configurations with rather low deformations ($\epsilon_2 \sim 0.15$); and (3) the bands consist of strong $M1$ transitions with only weak $E2$ crossovers resulting in large $B(M1)/B(E2)$ ratios [$\geq 20\mu_N^2/(eb)^2$]. These similarities have led to the suggestion that the bands might also be examples of the shears mechanism. Based on a weakly deformed prolate nuclear shape, the configurations in the Cd-Sn $M1$ bands now involve high- Ω $g_{9/2}$ proton holes and low- Ω $h_{11/2}$ neutron particles. TAC [22–24] and standard cranking [17–21] calculations have been able to reproduce experimental Routhians (energies in the rotating frame), angular momenta, and moments of inertia reasonably well. As discussed above, the behavior of the $B(M1)$'s should provide the discriminating test between these descriptions. In this Letter we report the results from an experiment we have performed to measure lifetimes of states in an $M1$ band in ^{110}Cd . Using the nomenclature of Ref. [20] the band of interest is labeled band 12.

High-spin states in ^{110}Cd were populated in the $^{96}\text{Zr}(^{18}\text{O}, 4n)$ reaction with a beam energy of 70 MeV.

The beam, accelerated by the 88-Inch Cyclotron of the Lawrence Berkeley National Laboratory, was incident on a target foil of $\approx 500 \mu\text{g}/\text{cm}^2$ ^{96}Zr (86% enrichment) backed with $\approx 10 \text{mg}/\text{cm}^2$ $^{\text{nat}}\text{Pb}$ to slow down and stop the recoils. Gamma rays were detected with the Gamma-sphere array [25] which for this experiment consisted of 99 large volume ($\sim 75\%$ efficient) Ge detectors situated at the following angles relative to the beam direction: five at 17.3° , five at 31.7° , five at 37.4° , nine at 50.7° , five at 58.3° , nine at 69.8° , four at 79.2° , three at 80.7° , eight at 90.0° , four at 99.3° , four at 100.8° , eight at 110.2° , five at 121.7° , ten at 129.9° , five at 142.6° , five at 148.3° , and five at 162.7° . A total of 9.95×10^8 events with fold four or higher (i.e., four or more coincident gamma rays) were collected. In addition, 4.97×10^8 events with fold four or higher were collected in a shorter run with a thin target of $\approx 500 \mu\text{g}/\text{cm}^2$ thickness.

The data were sorted into triple-gated, angle-dependent spectra and double-gated E_γ - E_γ correlation matrices. The thin-target data were used to extract accurate intensities and branching ratios. For the data taken with the Pb-backed target, Doppler-broadened line shapes were observed for in-band $M1$ transitions above the $I = 19$ state. Level lifetimes were extracted from these line shapes using the analysis package of Wells and Johnson [26]. The complete recoil-ion stopping was modeled using the prescription discussed in detail by Gascon *et al.* [27]. The tabulations of Northcliffe and Schilling [28] with shell corrections were used for the electronic stopping powers. The detailed slowing-down history of the recoils in the target and backing material was simulated using a Monte Carlo technique (5000 histories with a time step of 0.002 ps) and then sorted according to detector geometry. Calculated line shapes for each transition were obtained under the assumption that feeding into the top of the band was through a cascade of five transitions with the same moment of inertia as the in-band states. The topmost line shape was fitted and the extracted depopulation time was used as an input parameter to deduce lifetimes of states lower in the cascade. In addition, side feeding into each state was initially modeled as a rotational cascade of five transitions. The intensity of the side feeding was constrained to reproduce that observed experimentally (see Table I). The side-feeding lifetimes were always found to be shorter than the in-band lifetimes (up to 3 times shorter; the sensitivity of the fits to side-feeding variations in this range diminished for the states lower in the cascade). Simultaneous fits to forward, backward, and transverse spectra were performed. Final results were obtained from a global fit of the cascade with independently variable lifetimes for each state and the associated side feeding. Figure 1 shows the experimental data, along with calculated fits, for line shapes in the band of interest.

We obtained lifetimes for four states in the band. In addition, we assigned a new state to the top of the band which deexcites by a 869.3 keV transition. However, this line was too weak for us to extract an effective lifetime.

TABLE I. Measured lifetimes of states in the $M1$ band, τ (ps), and reduced transition strengths, $B(M1)$ (μ_N^2). I_{SF} is the percentage of side feeding into each state. The errors on the $B(M1)$ values were estimated from the standard (linear) transformation of the errors on the values of τ . Note, systematic errors introduced through the treatment of the stopping powers are not included.

E_γ (keV)	$I_i \rightarrow I_f$	I_{SF} (%)	τ (ps)	$B(M1)$ (μ_N^2)
372.4	20 \rightarrow 19	10(5)	$0.184^{+0.018}_{-0.022}$	$5.40^{+0.65}_{-0.53}$
462.5	21 \rightarrow 20	25(8)	$0.101^{+0.015}_{-0.018}$	$5.13^{+0.90}_{-0.75}$
562.5	22 \rightarrow 21	40(10)	$0.094^{+0.014}_{-0.018}$	$3.06^{+0.57}_{-0.45}$
673.3	23 \rightarrow 22	45(10)	$0.092^{+0.017}_{-0.023}$	$1.83^{+0.46}_{-0.34}$

The results are summarized in Table I. The quoted errors reflect the behavior of the χ^2 fit in the vicinity of the best value as the fit parameters were varied (including the side feeding). The errors do not include the systematic errors introduced through the treatment of the stopping powers; these may be as large as $\pm 20\%$.

Table I also gives the estimated $B(M1)$ transition rates deduced from the standard formula [29]. The $\Delta I = 1$ transitions were assumed to be of pure $M1$ character. No associated crossover $E2$ transitions could be firmly identified and so the $M1$ branching ratio was assumed to be 1.0. An experimental lower limit of $B(M1)/B(E2) \geq 60(\mu_N/eb)^2$ was deduced for the range of observed transitions.

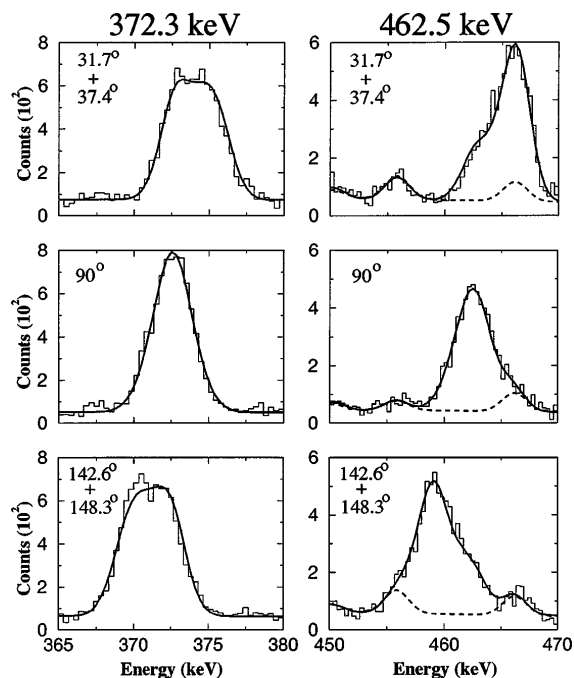


FIG. 1. Experimental data and associated line-shape fits for the 372.3 and 462.5 keV transitions of the band. The spectra were formed from a combination of clean gates on the stopped transitions in the cascade. The spectra are labeled by the angles at which the detectors were situated. The dashed line for the 462.5 keV line is the fit to small contaminant lines which interfere with the line shape.

In Fig. 2(a) we have plotted the angular momentum as a function of rotational frequency. It is clear that the sequence follows a near linear behavior of $I(\omega)$ which one would normally associate with a deformed rotational band. The solid curves in Fig. 2 are the results of a TAC calculation. (Note, the calculations do not extend to higher frequency since it becomes difficult to follow the correct configuration.) The suggested configuration for this band is $\pi g_{9/2}^{-2} \otimes \nu(h_{11/2}^2 \otimes AB)$, where we follow the standard cranking notation with AB representing the two lowest normal (positive) parity quasineutrons. The deformation parameters for this calculation were $\epsilon_2 = 0.13$ and $\gamma = 0^\circ$. These are self-consistent values found for $\hbar\omega = 0.3$ MeV. The value of the quadrupole-quadrupole coupling constant from [5] has been adopted and scaled as $A^{-5/3}$. Proton pairing was ignored due to the close proximity of the $Z = 50$ major shell closure. Neutron pairing effects were included by setting the pairing gap to a value of $\Delta_\nu = 1.1$ MeV which is appropriate for this region. The chemical potential, λ_ν , was fixed to ensure that the correct neutron number of $N = 62$ was obtained. Clearly, the calculations are able to reproduce the behavior of the band reasonably well.

Figure 2(b) is a plot of the experimentally deduced $B(M1)$ values (Table I) as a function of rotational frequency; there is good agreement between experiment and calculation. Both show the sharp decrease of the $B(M1)$ values with increasing spin in the band. This behavior is the clear signature of the shears mechanism. The decrease cannot be accounted for in standard rotational model approaches such as the Dönau and Frauendorf formalism

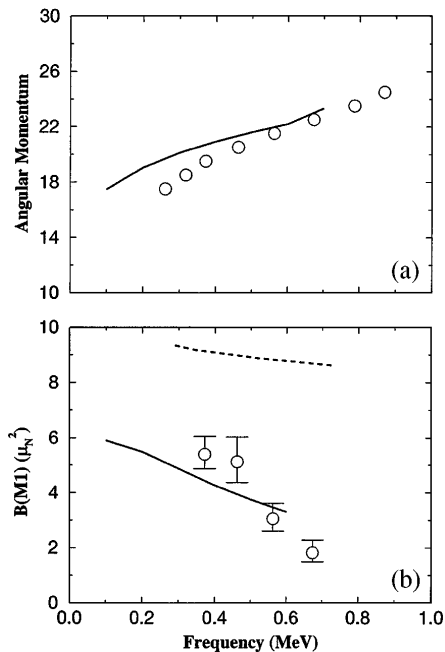


FIG. 2. Plots as functions of rotational frequency of (a) angular momentum, and (b) experimentally deduced $B(M1)$ values. The solid lines represent the result from the TAC calculations as described in the text.

[30] which assumes a fixed K value and that the alignment is perpendicular to the symmetry axis (i.e., no shears mechanism). The dashed line in Fig. 2(b) is the result of such a calculation for the $\pi g_{9/2}^{-2} \otimes \nu h_{11/2}^2$ configuration (including the normal-parity quasineutrons, of predominant $g_{7/2}$ and $d_{5/2}$ character, pushes the magnitude even higher). The gyromagnetic (g) factors of the $g_{9/2}$ protons and $h_{11/2}$ neutrons were taken to be 1.27 and -0.21 [31], respectively, while the rotational g -factor was assumed to be Z/A . It is clear that neither the magnitude nor slope can be reproduced. The empirical behavior of the $B(M1)$'s represents the first clear evidence of the shears mechanism in the $A \sim 110$ region.

We will now use the semiclassical approach of Macchiavelli *et al.* [15,16], which is based on a schematic model of the coupling of two long j vectors (\mathbf{j}_π and \mathbf{j}_ν), with the aim of extracting information on the effective interaction between the nucleons which are involved in the shears behavior. As shown in [15] the shears angle θ (the angle between \mathbf{j}_π and \mathbf{j}_ν) is the important degree of freedom in describing the bands and can be derived using the expression $\cos\theta = (I^2 - j_\pi^2 - j_\nu^2)/2j_\pi j_\nu$ where $j_\pi = 8$ and $j_\nu (= 15)$ is determined to reproduce the bandhead spin ($I_b = 17$), assuming a perpendicular coupling. The effect due to an increasing contribution from the core is taken into account by decomposing the total spin as $I = I_{\text{shears}} + R_{\text{core}}$, and using a linear relation $R_{\text{core}} = (\Delta R/\Delta I)(I - I_b)$, where $\Delta R/\Delta I$ is determined from the difference between the maximum observed spin ($I_{\text{max}} = 25$) and the sum of j_π and j_ν over the spin range ($\Delta I = 25 - 17 = 8$). Note, a recent analysis of the competition between the shears mechanism and the core rotation in a classical particles-plus-rotor model [32] validates decomposing the total angular momentum in this way. This contribution accounts for a maximum of $\leq 10\%$ of the total angular momentum at the top of the band. This is comparable to the small collective contribution to the total spin of the shears bands in the Pb nuclei [16].

Since $\geq 90\%$ of the angular momentum along the entire range of the band is generated through the shears mechanism we can make the reasonable approximation that the excitation energy along the band arises only by the change in potential energy caused by the recoupling of the two angular momentum vectors such that $V_{\pi\nu}[I(\theta)] = E(I) - E_b$. This allows us to extract the effective interaction between the neutrons in the neutron blade and the proton holes in the proton-hole blade. In Fig. 3 we plot the effective interaction between the two blades as a function of θ .

Following the analysis of Macchiavelli *et al.* [16], we expand the interaction in terms of even multipoles (thereby restricting ourselves to spatial forces) and assume for simplicity that we have a proton and neutron of the same j coupled to I and interacting via a term of the form $V_2 P_2(\theta)$. Since we have a particle-hole interaction, V_2 is positive. For comparison with the data we plot such a P_2 term in Fig. 3. The strong similarity between the two suggests

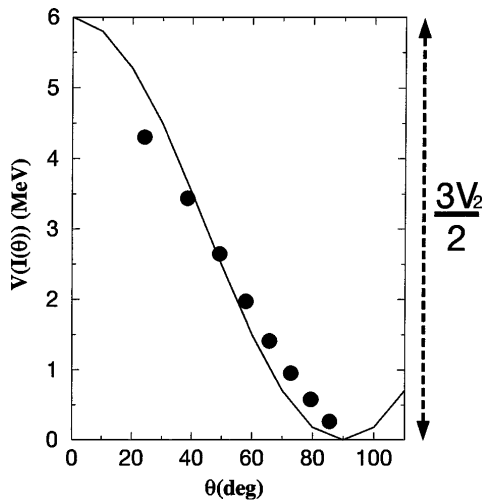


FIG. 3. The effective interaction between the angular momentum vectors, \mathbf{j}_π and \mathbf{j}_ν , as a function of shears angle. The solid curve is the expected dependence of a pure P_2 term in the interaction.

that a significant part of the interaction between the protons and neutrons may be represented by a P_2 interaction, just as in the case of the shears bands in the Pb nuclei. The strength of this interaction in the case of the band in ^{110}Cd is ~ 4 MeV. Taking into account two protons and four neutrons we estimate that the interaction strength per proton-hole/neutron pair is ~ 500 keV. These numbers are to be compared with values of ~ 2.3 MeV and ~ 300 keV, respectively, for the shears bands in ^{198}Pb . One would expect the interaction to scale as $1/A$, which we indeed find from the values given above.

To summarize, we have performed an experiment with the Gammasphere array to measure the lifetimes of states in a rotational-like $M1$ band in ^{110}Cd through the fitting of Doppler-broadened line shapes. The band is clearly an example of a shears band. This is the first definitive result indicating that the shears mechanism (and magnetic rotation) is operative in the $A \sim 110$ region. Using a semiclassical analysis of the coupling of two long angular momentum vectors we have shown that the collective contribution of the core in generating the total angular momentum is small ($\leq 10\%$) and that the main ingredient to the effective interaction between the constituent nucleons forming the blades follows a P_2 -type term with a strength of ~ 500 keV. The properties of this band are strikingly similar to the shears bands in the Pb nuclei suggesting a common origin of the mechanism in both mass regions. It has been suggested that the origin of the interaction may be from a particle-quadrupole vibration coupling [16]. However, no quantitative calculations of this sort have been performed to date and we hope that the data and analysis presented in this Letter will spur theoretical effort in this direction.

We express our gratitude to Dr. John Wells for providing us with the latest version of the line-shape codes, and to the crew and staff of the 88-Inch Cyclotron for superb operation. This work has been supported in part by the U.S. DoE under Contract No. DE-AC03-76SF00098 (LBNL). Funding from the U.K. came from the EPSRC.

*Present address: W. A. Wright Nuclear Structure Laboratory, Physics Department, Yale University, P.O. Box 208124, New Haven, CT 06520.

†Present address: Department of Physics, University of Manchester, Manchester M13 9PL, UK.

- [1] R. M. Clark *et al.*, Phys. Lett. B **275**, 247 (1992).
- [2] G. Baldsiefen *et al.*, Phys. Lett. B **275**, 252 (1992).
- [3] A. Kuhnert *et al.*, Phys. Rev. C **46**, 133 (1992).
- [4] G. Baldsiefen *et al.*, Nucl. Phys. **A592**, 365 (1995), and references therein.
- [5] S. Frauendorf, Nucl. Phys. **A557**, 259c (1993).
- [6] G. Baldsiefen *et al.*, Nucl. Phys. **A574**, 521 (1994).
- [7] T. F. Wang *et al.*, Phys. Rev. Lett. **69**, 1737 (1992).
- [8] J. R. Hughes *et al.*, Phys. Rev. C **48**, R2135 (1993).
- [9] E. F. Moore *et al.*, Phys. Rev. C **51**, 115 (1995).
- [10] M. Neffgen *et al.*, Nucl. Phys. **A595**, 499 (1995).
- [11] R. M. Clark *et al.*, Phys. Rev. Lett. **78**, 1868 (1997).
- [12] R. M. Clark *et al.*, Phys. Lett. B **440**, 251 (1998).
- [13] R. Krücken *et al.*, Phys. Rev. C **58**, R1876 (1998).
- [14] S. Frauendorf, in *The Proceedings of the Conference on Physics from Large Gamma-Ray Detector Arrays, Berkeley, 1994* [Report No. LBL-35687, Vol. 2, p. 52].
- [15] A. O. Macchiavelli *et al.*, Phys. Rev. C **57**, R1073 (1998).
- [16] A. O. Macchiavelli *et al.*, Phys. Rev. C **58**, R621 (1998).
- [17] I. Thorslund *et al.*, Nucl. Phys. **A564**, 285 (1993).
- [18] I. Thorslund *et al.*, Nucl. Phys. **A568**, 306 (1994).
- [19] P. H. Regan *et al.*, Phys. Rev. C **49**, 1885 (1994).
- [20] S. Juutinen *et al.*, Nucl. Phys. **A573**, 306 (1994).
- [21] R. Wadsworth *et al.*, Phys. Rev. C **50**, 483 (1994).
- [22] A. Gadea *et al.*, Phys. Rev. C **55**, R1 (1997).
- [23] D. G. Jenkins *et al.*, Phys. Lett. B **428**, 23 (1998).
- [24] S. Frauendorf, in *Proceedings of the Workshop on Gammasphere Physics, Berkeley*, edited by M. A. Deleplanque, I. Y. Lee, and A. O. Macchiavelli (World Scientific, Singapore, 1995), p. 272.
- [25] I. Y. Lee, Nucl. Phys. **A520**, 641c (1990).
- [26] J. C. Wells and N. Johnson (private communication). Modified from the original code by J. C. Bacelar.
- [27] J. Gascon *et al.*, Nucl. Phys. **A513**, 344 (1990).
- [28] L. C. Northcliffe and R. F. Schilling, Nucl. Data Tables **7**, 233 (1970).
- [29] H. Ejiri and M. J. A. de Voigt, *Gamma Ray and Electron Spectroscopy in Nuclear Physics* (Oxford University Press, Oxford, England, 1987), p. 504.
- [30] F. Dönau and S. Frauendorf, in *Proceedings of the International Conference on High Angular Momentum Properties of Nuclei, Oak Ridge, 1982*, Nucl. Sci. Res. Conf. Series Vol. 4 (Harwood, New York, 1983), p. 143.
- [31] T. Lonnröth *et al.*, Z. Phys. A **317**, 215 (1984).
- [32] A. O. Macchiavelli *et al.* (to be published).